Mol Neurobiol
DOI 10.1007/s12035-013-8530-7

Rat Cerebellar Slice Cultures Exposed to Bilirubin Evidence Reactive Gliosis, Excitotoxicity and Impaired Myelinogenesis that Is Prevented by AMPA and TNF-α Inhibitors

Andreia Barateiro · Helena Sofia Domingues · Adelaide Fernandes · João Bettencourt Relvas · Dora Brites

Received: 10 May 2013 / Accepted: 5 August 2013

Abstract The cerebellum is one of the most affected brain regions in the course of bilirubin-induced neurological dysfunction. We recently demonstrated that unconjugated bilirubin (UCB) reduces oligodendrocyte progenitor cell (OPC) survival and impairs oligodendrocyte (OL) differentiation and myelination in co-cultures of dorsal root ganglia neurons and OL. Here, we used organotypic cerebellar slice cultures, which replicate many aspects of the in vivo system, to dissect myelination defects by UCB in the presence of neuroimmune-related glial cells. Our results demonstrate that treatment of cerebellar slices with UCB reduces the number of myelinated fibres and myelin basic protein mRNA expression. Interestingly, UCB addition to slices increased the percentage of OPC and decreased mature OL content, whereas it decreased Olig1 and increased Olig2 mRNA expression. These UCB effects were associated with enhanced gliosis, revealed by an increased burden of both microglia and astrocytes. Additionally, UCB treatment led to a marked increase of tumor necrosis factor (TNF)-α and glutamate release, in parallel with a decrease of interleukin (IL)-6. No changes were observed relatively to IL-1β and S100B secretion. Curiously, both α-amino-3-hydroxy-5-methyl-4-isoxazolepropionic acid (AMPA) receptor antagonist and TNF-α antibody partially prevented the myelination defects that followed UCB exposure. These data point to a detrimental role of UCB in OL maturation and myelination together with astrocytosis, microgliosis, and both inflammatory and excitotoxic responses, which collectively may account for myelin deficits following moderate to severe neonatal jaundice.

Keywords Astrocytes · Cerebellar slice culture · Microglia · Myelination · Oligodendrocytes · Unconjugated bilirubin

A. Barateiro · A. Fernandes (✉) · D. Brites
Research Institute for Medicines and Pharmaceutical Sciences (iMed.UL), Faculdade de Farmácia, Universidade de Lisboa, Av. Professor Gama Pinto, 1649-003 Lisbon, Portugal
e-mail: amaf@ff.ul.pt

D. Brites
e-mail: dbrites@ff.ul.pt

H. S. Domingues · J. B. Relvas
Instituto de Biologia Molecular e Celular, University of Porto, Rua do Campo Alegre 823, 4150-180 Porto, Portugal

A. Fernandes · D. Brites
Department of Biochemistry and Human Biology, Faculdade de Farmácia, Universidade de Lisboa, Av. Professor Gama Pinto, 1649-003 Lisbon, Portugal

Introduction

Neonatal jaundice is one of the most common clinical situations in pediatrics. The condition derives from an abnormal elevation of circulating unconjugated bilirubin (UCB) together with a defective clearance during the first days after birth. The risk for developing bilirubin-induced neurologic dysfunction (BIND) and *kernicterus* depends on the degree of mismatch between bilirubin production and elimination [1, 2]. BIND develops when the level of serum UCB exceeds the bilirubin binding capacity of albumin and unbound UCB increasingly crosses the blood-brain barrier [3] surpassing the protective mechanisms of the brain designed to prevent UCB accumulation [4]. Indeed, UCB has been detected within neurons in brain sections of icteric infants [5], in parallel with neuronal loss, astrogliosis and microgliosis [6]. Interestingly, recent data have shown loss of myelinated fibres in cerebellar sections from a pre-term infant with *kernicterus* [7]. Moreover, a reduction of white matter (WM) volume and delay in hemispheric myelination was reported in infants at risk of BIND [8].

In BIND, UCB can cause cell death by both apoptosis and necrosis, depending on the concentration and duration of the interaction of UCB with the cells, as well as on the cell type involved [9–11]. In addition, UCB promotes glutamate release by both neurons and astrocytes [12, 13], which triggers excitotoxicity and neuronal death as treatment with the

Published online: 28 August 2013

N-methyl-D-aspartate receptor (NMDA) antagonist MK-801 prevented such outcome [14, 15].

Inflammation also plays an important role in brain damage by UCB. Indeed, UCB has immunostimulant properties on both astrocytes and microglia, leading to the release of the pro-inflammatory cytokines tumor necrosis factor (TNF)-α and interleukin (IL)-1β [12, 16–18]. Although treatment of rat neuron primary cultures with UCB elicited a small secretion of TNF-α, no cytokine release was observed when hippocampal slice cultures were used instead [13, 19]. In addition, our own and other studies have demonstrated that UCB damage to developing neurons involves neuritic atrophy, neuronal arborisation reduction, neuritic growth arrest and neuritic hypoplasia [20, 21]. Furthermore, we have recently shown that UCB reduces both the survival of oligodendrocyte progenitor cells (OPC) through mitochondrial dysfunction and endoplasmic reticulum stress [22] and the ability of the remaining oligodendrocytes (OL) to differentiate and maturate, causing a deficient myelination when co-cultured with dorsal root ganglia (DRG) neurons [23].

We have developed experimental in vitro cellular models, commonly used to understand the process of myelination, to identify and characterise specific pathways and mechanisms by which UCB toxicity affects OL survival and development. However, as UCB activates microglia and astrocytes, and these cells play an important role in inflammation, synapse development and physiology [24–26], here, we decided to study UCB effects in organotypic cultures. Such cultures provide an experimental setting that replicates well the complex multicellular environment, preserving cell relationships and maintaining extracellular matrix in a relatively intact three-dimensional structure [11]. In addition, it has been shown that organotypic cultures avoid several sources of artefacts and misinterpretations [27, 28], thus allowing reproducible treatments. Moreover, the use of cerebellar organotypic slices may be particularly appropriated to evaluate injury by UCB, once it is one of the most affected brain regions in BIND [29, 30]. Most importantly, mouse cerebellar slice cultures contain both OPC and mature OL and form compact myelin [31], reinforcing the suitability of this model to study the dramatic morphological and biochemical changes [32] associated with OL maturation and myelination. To this, it may account the role of Olig1 and Olig2, key transcription factors in OL lineage specification through their progressive stages of maturation until myelination. While Olig1 appears to be mostly implicated in OL maturation, being involved in the final stages of myelin production [33, 34], Olig2 is required for the development of OPC [33, 35]. It is well established that OL undergo four distinct differentiation stages: OPC that express markers like NG2 proteoglycan, late progenitors that express the sulfatide O4, immature OL expressing galactosylceramidase and finally mature OL that express myelin proteins, such as myelin basic protein (MBP) [36]. These myelin proteins are required not only for the saltatory conduction of neuronal action potentials but also for maintenance of axonal integrity and fast axonal transport [37].

Interestingly, several studies have demonstrated that the toxic effects of increased extracellular concentration of glutamate are maturation dependent, being more prominent in OPC or in immature OL than in mature OL [38–40]. In addition, it was reported that α-amino-3-hydroxy-5-methyl-4-isoxazolepropionic acid (AMPA) receptor in OL lack GluR2 subunit and therefore are Ca^{2+} permeable, which has a crucial relevance for the damaging actions of glutamate on OL [41]. In this context, a recent study has demonstrated that NMDA receptor-deficient OPC proliferate normally, achieve appropriate densities in grey, and WM tracts immediately, maintaining their physiological and morphological properties and their ability to establish synapses with glutamatergic axons [42].

In this study, we aimed to evaluate the effect of UCB on the rat cerebellar slice culture model by dissecting myelination and glial reactivity. Our findings indicate that treatment of rat cerebellar slice cultures with UCB leads to a long-lasting reduction in the percentage of myelinated fibres. This myelination deficit was corroborated by a decrease in MBP mRNA expression, and paralleled by an increase in the number of OPC (NG2+ cells). The downregulation of Olig1 and upregulation of Olig2 by UCB further reinforces its interference in OL differentiation process. Sustained microgliosis and astrocytosis were also observed in slices treated with UCB as compared with vehicle-treated ones. UCB promoted a rapid and sustained release of TNF-α and a transient increase of extracellular glutamate levels while decreasing IL-6 secretion. IL-1β and S100B production was not different from vehicle-treated slices. Importantly, an antibody directed to TNF-α and an AMPA receptor antagonist prevented UCB-induced impairment of neuronal fibres and myelination. Overall, our data demonstrate that in addition to myelination deficits and OL differentiation impairment, UCB concomitantly causes gliosis and inflammation, which may have detrimental roles in the jaundiced newborn, namely in persistent unconjugated hyperbilirubinemia.

Materials and Methods

Reagents and Media

Minimum essential medium Eagle (MEM), D-(+)-glucose solution 45 % and bovine serum albumin fraction V (BSA; fraction V, fatty acid free), rabbit anti-glial fibrillary acidic protein (GFAP; #G9269), monoclonal anti-S100B capture antibody (#S2532) and the AMPA receptor antagonist 6-cyano-7-nitroquinoxaline-2,3-dione (CNQX) were purchased from Sigma (St. Louis, MO, USA). UCB was also obtained from Sigma and purified according to the method of McDonagh [43]. Normal horse serum (NHS), Hank's buffered salt solution

(HBSS), 50 U mL penicillin 50 μg^{-1} mL^{-1} streptomycin and L-glutamine were acquired from Gibco (Life Technologies, Inc., Grand Islands, USA). Cell culture inserts for 6-well plates with 0.4 μm pores, translucent, high-density PET membrane were from BD Falcon (#353493, Lincoln Park, NJ, USA). Rabbit antibody anti-NG2 was from Millipore (#AB5320, Billerica, MA, USA). Rat antibody anti-MBP was purchased from AbD Serotec (#MCA409S, Raleigh, NC, USA). Mouse antibody anti-neurofilament-medium [NF-09] was from Abcam (#ab7794, Cambridge, UK). Rabbit anti-ionised calcium-binding adaptor molecule 1 (Iba-1) was purchased from Wako (#019-19741, Osaka, Japan). Alexa Fluor 488 goat anti-mouse IgG, Alexa Fluor 568 goat anti-rat IgC, Alexa Fluor 488 goat anti-rabbit IgG were acquired from Invitrogen Life Sciences (Carlsbad, CA, USA). Policlonal anti-S100B detection antibody was from Dako (#Z0311, Glostrup, Dennmark). Direct-Zol™ RNA MiniPrep was obtained from Zymo Research (Irvine, CA, USA). RevertAid H Minus First Strand cDNA synthesis and Maxima SYBR Green qPCR Master Mix (2×) were acquired from Fermentas (Ontario, Canada, USA). Recombinant rat TNF-α, IL-1β and IL-6 and DuoSet® ELISA kits and anti-rat TNF-α antibody were from R&D Systems, Inc. (Minneapolis, MN, USA). L-glutamic acid kit was from Roche Molecular Biochemicals (Mannheim, Germany). Shandon Immu-Mount™ aqueous non-fluorescing mounting medium was acquired from Thermo Scientific (Waltham, MA, USA).

Animals

Wistar rats were maintained on a 12-h light/dark cycle under conditions of constant temperature and humidity. Animals were supplied with standard laboratory chow and water ad libitum. Animal care followed the recommendations of the European Convention for the Protection of Vertebrate Animals Used for Experimental and Other Scientific Purposes (Council Directive 86/609/EEC) and National Law 1005/92 (rules for protection of experimental animals). All animal procedures were approved by the Institutional Animal Care and Use Committee. All efforts were made to minimise animal suffering, to reduce the number of animals used and to use alternatives to in vivo techniques.

Cerebellar Slice Culture

Cerebellum parasagittal slices were prepared from postnatal day (P) 7 Wistar rat brains using entire littermates, according to the interface culture method. Briefly, rats were decapitated and the cerebellum was extracted in ice-cold HBSS. Then, 400 μm slices were made using a McIlwain tissue chopper, separated in culture medium and selected for clear cerebellar morphology. Four slices of different animals were placed in each upper chamber of a 0.4-μm pore cell culture insert. Cultures were maintained in 6-well culture plates containing 1 mL of medium in the plate well, at 37 °C, in room air and with 5 % CO_2 for 7 days in vitro (DIV). The culture medium consisted of 50 % MEM, 25 % HBSS, 25 % NHS, 6.5 mg/mL D-glucose and 0.5 % penicillin/streptomycin. Half of the medium was replaced every day. Rat P7 cerebellar slices were not completely myelinated when placed in culture. During the time in culture, OL differentiation occurred until they filled the WM of folia and started myelination. After 7 DIV, the cerebellar slice culture evidenced a high degree of myelination, based on the significant acquirement of the number of myelin processes aligned with axons. The slice thickness reduced with time in culture and showed three distinct regions in the Z plane that were different in their cellular composition and appearance: the first 1-5 μm ('top') presented the majority of the myelin, axons, OL, OPC and astrocytes reside; the next 6-23 μm ('middle') had the same composition as the 'top' layer, however at lesser amounts; the last 24-30 μm ('bottom') was mostly devoid of all cellular components except microglia, which were also found throughout other depths of the slice albeit at lower levels.

Slice Culture Treatments

To evaluate the effect of UCB in the de novo myelination, P7 cerebellar slices were kept in culture for 3 DIV to allow the clearance of debris and the stabilisation of the system. After 3 DIV, prior to the emergence of compact myelin that occurs at 7 DIV, four to five different wells, containing four slices from distinct animals, were incubated with UCB (Fig. 1a). UCB-induced alterations were measured along the incubation or at the end of in vitro culture at 7 DIV and either one slice or the culture media of each well was considered $n=1$. Exposure of slices to UCB for 8 and 24 h aimed to mimic a more acute (first) or chronic (second model) condition, respectively.

Normally, we use a stable solution of UCB/human serum albumin (HSA)=0.5 [44] to avoid the formation of UCB oligomers, microaggregates and even precipitates, which occur at higher molar ratios due to the increased levels of unbound (non-albumin bound or 'free') bilirubin that surpasses 70 nM in aqueous solution [45, 46]. This UCB/HSA solution was shown to produce a concentration of free bilirubin of 20 nM [50], which was previously observed in jaundiced newborns with serum bilirubin levels between 116 and 615 μM and ≥2.5 kg birth weight [49]. With this model, we have demonstrated that UCB produces cell membrane destruction [47, 48] and injurious effects on oligodendrogenesis and myelinogenesis [22, 23]. In the present experimental system, as the presence of a high concentration of NHS, also containing albumin, was indispensable for the maintenance of cerebellar slice cultures, we assayed the conditions needed to give the same amount of 20 nM of free bilirubin. Therefore, instead of 50 μM UCB in the presence of 100 μM HSA, as indicated in our previous reports, cultures were here treated with 60 μM UCB in the

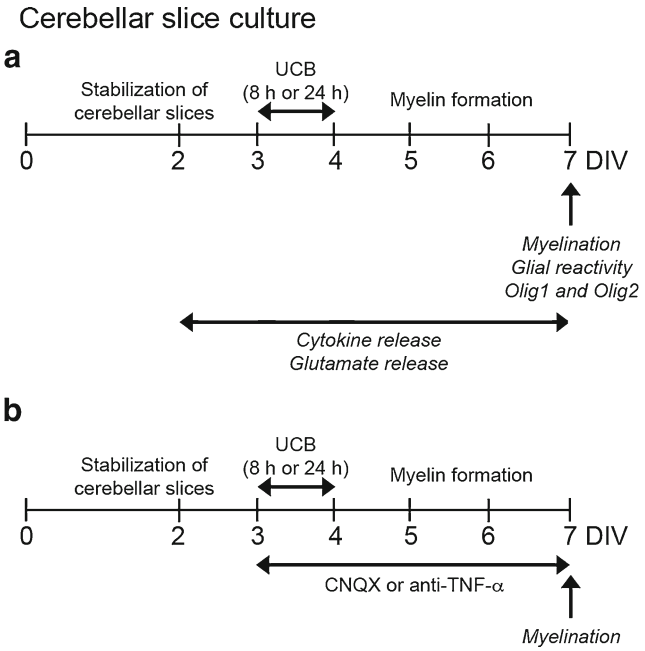

Fig. 1 Schematic representation of the conditions and timeline used to assess the alterations caused by unconjugated bilirubin (*UCB*) in cerebellar slice cultures. Slices were obtained from postnatal day 7 Wistar rat cerebellum and kept in culture for 3 days in vitro (*DIV*), to allow the clearance of debris and the stabilisation of cerebellar slices. **a** Slices were incubated in the absence (vehicle) or in the presence of UCB for 8 and 24 h at 37 °C to mimic acute (first) and chronic (second model) hyperbilirubinemia, respectively. Following UCB exposure, the incubation media was replaced with cerebellar slice culture media and slices were analysed at 7 DIV to assess the extent of myelination, glial reactivity and Olig1 and Olig2 mRNA expressions. In addition, cytokine and glutamate release were evaluated immediately before and after UCB treatment and in the following days until the cultures reached 7 DIV. **b** In parallel experiments, cerebellar slice cultures were incubated with UCB for 8 and 24 h plus the specific AMPA receptor antagonist 6-cyano-7-nitroquinoxaline-2,3-dione (*CNQX*) or the anti-rat tumor necrosis factor (*TNF*)-α till the 7 DIV, the time point to evaluate myelination

presence of 25 % of NHS. In this condition, we reproduced the 20 nM of free bilirubin, thus avoiding the marked nerve cell death [10], with impairment of cellular membranes [48], cytoskeleton [10] and important cellular functions [10] triggered by higher free bilirubin levels.

All UCB solutions were prepared from a 10 mM stock solution in 0.1 N NaOH immediately before use and the pH of the incubation media was restored to 7.4 by addition of equal amounts of 0.1 N HCl. All the experiments with UCB were performed under light protection to avoid photodegradation. After incubation, the UCB containing medium was removed and replaced with fresh culture medium.

To assay the role of glutamate and TNF-α on UCB-induced effects, cerebellar slice cultures were incubated with 10 μM of the specific AMPA receptor antagonist CNQX, or with 0.15 μM anti-rat TNF-α in combination with UCB during 8 or 24 h as described above. As the levels of glutamate and specially TNF-α were still elevated following incubation, we decided to keep both compounds in the culture medium until the end of the culture, at 7 DIV (Fig. 1b).

Immunostaining Procedure

After 7 DIV, cerebellar slice cultures were fixed with 4 % paraformaldehyde in phosphate-buffered saline (PBS; pH 7.4) for 30 min at room temperature. Membranes containing tissue sections were cut out from cell culture insert and incubated with blocking solution (1 nM 4-(2-hidroxyethyl)-1-piperazineethanosulfonic, 2 % heat-inactivated horse serum, 10 % heat-inactivated goat serum, 1 % BSA, and 0.25 % Triton X-100 in HBSS) for 3 h to block non-specific binding. The sections were incubated with primary antibodies diluted in blocking solution for 24 h at 4 °C. The following antibodies were used: neurofilament-medium [NF-09] for neuronal axons (1:50), NG2 for OPC (1:100), MBP for mature OL (1:50), GFAP for astrocytes (1:250) and Iba-1 for microglia (1:250). The next day, slices were washed three times for 30 min each with PBS before incubation for another 24 h at 4 °C with secondary antibody in blocking solution (1:1,000). Slices were then washed three times for 30 min and mounted for confocal microscopy. Percentage of the area immunoreactive for each antibody was measured in ×40 magnification images acquired in a Laser Scanning Confocal Microscope Leica SP2 AOBS SE (Leica Microsystems, Germany). The range of the slice was determined using Z-stack imaging at 1-μm intervals and a series of images derived from Z-stack imaging were analysed. Briefly, binary masks were defined using the same cut-off intensity threshold value for each region of interest, which corresponds to each cell immunostained, defined as the minimum intensity because of specific staining above background values. Then, the percentage of the area occupied by neurofilaments, MBP, NG2, GFAP and Iba-1 were measured automatically using ImageJ software in each cerebellum region. Results are given by averaging values determined in at least seven separate microscopic fields from slices of four different animals.

Semiquantitative RT-PCR

Total RNA was extracted from each tissue section after 7 DIV using Direct-Zol™ RNA MiniPrep kit, according to the manufacturer's instructions. Total RNA was quantified using Nanodrop ND-100 Spectrophotometer (NanoDrop Technologies, Wilmington, DE, USA). Aliquots of 1 μg of total RNA were treated with DNase I and then reverse transcribed into cDNA using oligo-dT primers and SuperScript II Reverse Transcriptase under the recommended conditions. Quantitative RT-PCR (qRT-PCR) was performed using glyceraldehyde-3-phosphate dehydrogenase (GAPDH) as an endogenous control to normalise the expression level of Olig1 and Olig2

transcription factors. The following sequences were used as primers: Olig1 sense 5′-GCCCAGGCCACGAGTACAAA-3′ and anti-sense 5′-TCCACTCCGAAACCCAACGA-3′ [51]; Olig2 sense 5′-GAAATGGAATAATCCCGAACTACT-3′ and anti-sense 5′-CCCCTCCCAAATAACTCAAAC-3′ [51]; GAPDH sense 5′-TGGAGTCTACTGGCGTCTT-3′ and anti-sense 5′-TGTCATATTTCTCGTGGTTCA-3′. qRT-PCR was performed on a real-time PCR detection (Applied Biosystems 7300 Fast Real-time PCR System, Applied Biosystem, Madrid, Spain) using a SYBR Green qPCR Master Mix. The PCR was performed in 96-well plates with each sample performed in triplicate, and a no-template control was included for each amplification product. qRT-PCR was performed under optimised conditions: 94 °C for 3 min followed by 40 cycles at 94 °C for 9 s, 60 °C for 12 s and 72 °C for 9 s. To verify the specificity of the amplification, a melt-curve analysis was performed, immediately after the amplification protocol. Non-specific products of PCR were not detected in any case. Relative mRNA concentrations were calculated using the Pfaffl modification of the $\Delta\Delta C_T$ equation (cycle number at which fluorescence passes the threshold level of detection (C_T)), taking into account the efficiencies of individual genes. The results were normalised to GAPDH in the same sample and the initial amount of the template of each trial was determined as relative expression by the formula $2^{-\Delta\Delta CT}$. ΔC_T is the value obtained, for each sample, by performing the difference between the mean C_T value of each Olig gene and the mean C_T value of GAPDH. $\Delta\Delta C_T$ of one sample is the difference between its ΔC_T value and the ΔC_T of the sample chosen as reference, in our case the vehicle-treated cells.

Glutamate Determination

Release of glutamate to the culture medium was determined following UCB exposure and along the time-course of the experiments by an adaptation of the L-glutamic acid kit (Roche), using a 10-fold volume reduction [12]. The reaction was performed in a 96-well microplate and the absorbance measured at 490 nm. A calibration curve was used for each assay. All samples and standards were analysed in duplicate. Results are expressed in μM.

Cytokine Determination

Cytokine release by cerebellar slice cultures was quantified following UCB exposure and along the time-course of the experiments. Aliquots of the slice culture media were placed in a 96-well microplate and assessed, in duplicate, for TNF-α, IL-1β and IL-6 with specific DuoSetR ELISA Development kits, according to the manufacturer's instructions. Measurements were performed at 450 nm, with a reference filter at 620 nm, using a microplate reader. Results are expressed as picogrammes per millilitre.

S100B Determination

S100B release to the culture media was determined by ELISA as usual in our laboratory [52]. Briefly, culture media were incubated for 2 h at 37 °C on a 96-well plate previously coated with a monoclonal anti-S100B antibody (1:1,000). Thereafter, a polyclonal anti-S100B antibody (1:5,000) was added and samples additionally incubated for 30 min at 37 °C. Finally, an anti-rabbit peroxidase-conjugated antibody (1:5,000) was added for further 30 min at 37 °C. The colorimetric reaction with Sigma Fast OPD tablets was measured at 492 nm, using a microplate reader. Results are expressed in nanogrammes per millilitre.

Statistical Analysis

Results of, at least, four different experiments are expressed as mean±SEM. Significant differences between groups were determined by one-way ANOVA and Bonferroni post hoc test. To compare the effects of UCB treatment and time of incubation two-way ANOVA was used with UCB treatment and time of incubation as between-subjects factors using GraphPad Prism® 5.0 (GraphPad Software, San Diego, CA, USA).

Results

UCB Impairs Myelination in Rat Cerebellar Slice Cultures

In the present study, we decided to evaluate the noxious effects of UCB in the cerebellum, one of the brain regions most affected in *kernicterus* [7]. To do this, we used cerebellar slice cultures, a model closer to the in vivo situation and commonly employed in the evaluation of myelination [31]. Our interest was supported by previous studies showing that UCB reduces OPC survival [22] and compromises myelinogenesis [23].

Cerebellar slice cultures were treated, at 3 DIV, with UCB during 8 and 24 h and maintained in culture until 7 DIV. Then, slices were immunostained for neurofilaments and MBP in order to determine the number of axons and the percentage of myelinated fibres. As neuronal loss can impair myelination, we first determined the percentage of area occupied by neurofilaments. As depicted in Fig. 2a, b, both periods of UCB treatment led to a significant decrease in the percentage of area occupied by neurofilaments (0.74±0.05-fold at 8 h and 0.68±0.07-fold at 24 h; Bonferroni $P<0.01$), indicating that UCB treatment, rather than time of incubation, affects neuronal arborisation. Thus, we next determined the percentage of myelinated fibres to correct for the lower levels of fibres presented in UCB-treated slices. Interestingly, the treatment with UCB induced a time-dependent decrease in the percentage of myelination of the remaining fibres (0.70±0.02-fold at 8 h and 0.48±0.02-fold at 24 h, Bonferroni $P<0.01$, ANOVA UCB treatment×time of incubation F 55.29, $P<0.001$), as

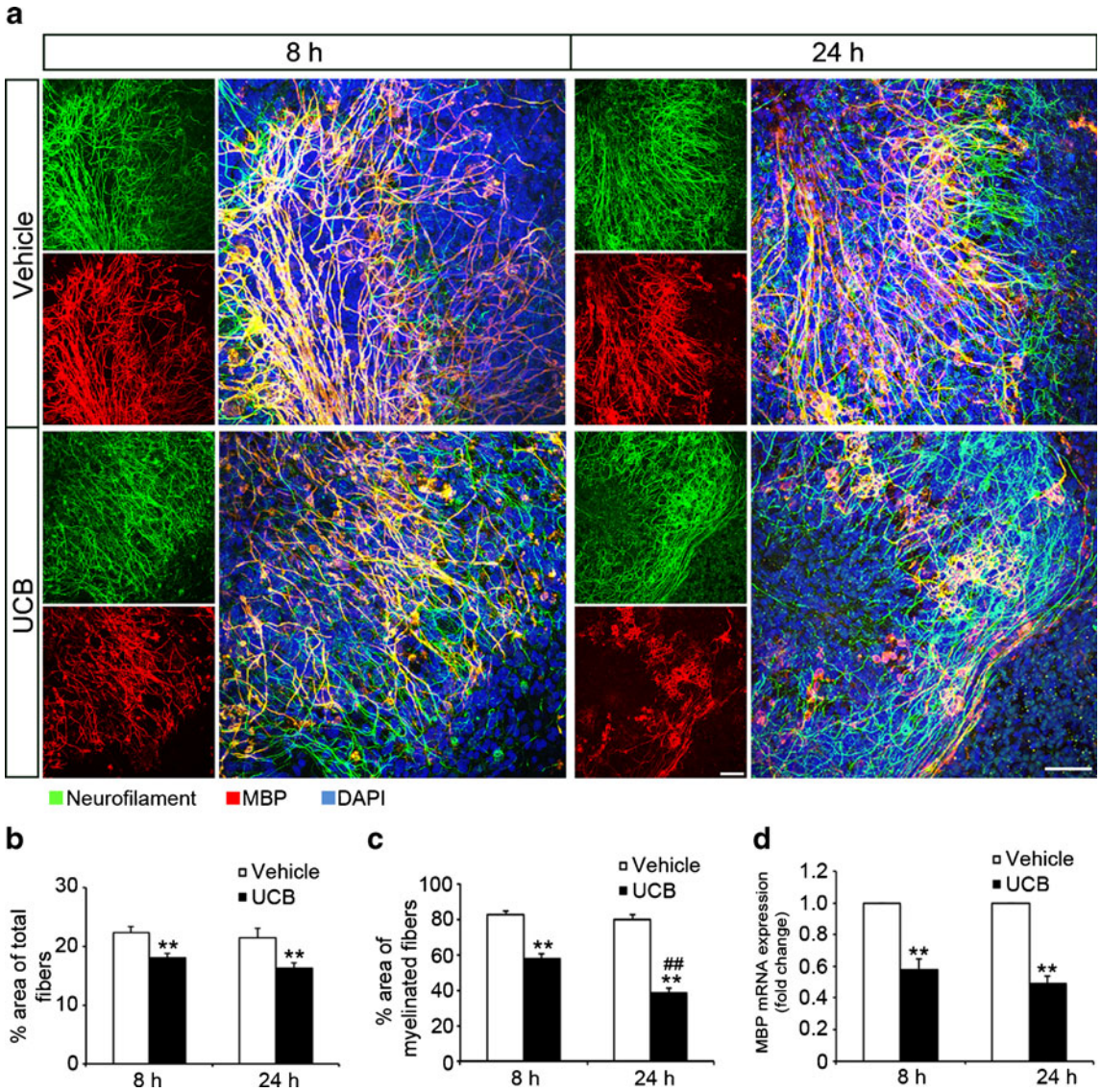

Fig. 2 Unconjugated bilirubin (*UCB*) impairs myelination, with increasing effects along the time of exposure. Rat cerebellar slice cultures were exposed to UCB at 3 DIV for 8 and 24 h and allowed to recover until 7 DIV. **a** OL were immunolabeled for myelin basic protein (*MBP*; *red*) to detect myelinated tracts and neurofilaments (*NF*; *green*) to detect neuronal axons. Nuclei were counterstained with DAPI dye (*blue*). Representative images show reduced myelination after 8 h incubation with UCB (*left column*), which further decreased at 24 h (*right column*). Percentage of the total area occupied by neurofilaments (**b**), and percentage of the area occupied by myelinated fibres (**c**) from sections of four distinct animals. **d** Relative MBP mRNA levels determined by qRT-PCR with the $\Delta\Delta C_T$ method. Values are shown as mean±SEM from five sections of distinct animals, performed in triplicate and normalised to values measured for glyceraldehyde 3-phosphate dehydrogenase in the same samples. *Scale bar* represents 50 μm. $^{**}P<0.01$ vs. respective vehicle; $\#\#P<0.01$ vs. 8 h of UCB exposure

observed by a reduction in the number and length of the internodes (Fig. 2a, c). This observation was corroborated by the similar pattern in the decrease of MBP mRNA expression obtained for both treatments (Fig. 2d), with a slight more evident reduction at 24 h as compared with 8 h treatment (0.57±0.06-fold for 8 h and 0.48±0.05-fold for 24 h; Bonferroni $P<0.01$). These data suggest that early exposure to UCB affects neuronal arborisation in this model, but even more OL ability to myelinate axons. Time of exposure increased the magnitude of the myelination effect. Although our cerebellar slice cultures already contain at 3 DIV some myelinated fibres, we did not observe any sign of myelin debris at 7 DIV, indicating that UCB rather than destroying the formed myelin is preventing myelin de novo formation.

Impairment of Myelination by UCB Is Associated with Reduced OL Differentiation

We have previously shown that UCB affects OL differentiation and maturation with consequent myelination impairment in a DRGneuron-OL co-culture system [23]. Thus, we hypothesised that a reduction of OL differentiation accounting for the lower

percentage of myelinated fibres could also be occurring in the organotypic culture system. To address this issue we next immunostained the cerebellar slices with NG2 to identify OPC, and with MBP to detect both mature OL and myelinated fibres. As depicted in Fig. 3a, b, cerebellar slices exposed to UCB exhibited an increased area occupied by NG2+ cells, slightly enhanced when UCB treatment was more prolonged (2.26±0.58-fold at 8 h and 2.62±0.66-fold at 24 h; Bonferroni $P<0.01$). As expected, given our previous results, the area of MBP was dramatically decreased in the cerebellar slices treated with UCB when compared with vehicle-treated ones (Fig. 3a, c), even more markedly after 24 h exposure to UCB (0.51±0.12-fold at 8 h and 0.36±0.04-fold at 24 h, Bonferroni $P<0.01$). These results show that exposure to UCB, in a neurodevelopmental period in which OPC have not yet differentiated to mature OL (3 DIV), inhibits OPC differentiation, explaining the significant increase in the percentage of immature NG2+ OPC and the decrease in the percentage of mature MBP+ OL we have observed.

Delay in OL Maturation by UCB Is Supported by Changes in Olig1 and Olig2 mRNA Expressions

Olig1 and Olig2 are transcription factors playing essential roles in the differentiation of the OL lineage, from glial precursor cells to fully mature myelinating OL [53–56]. We have recently

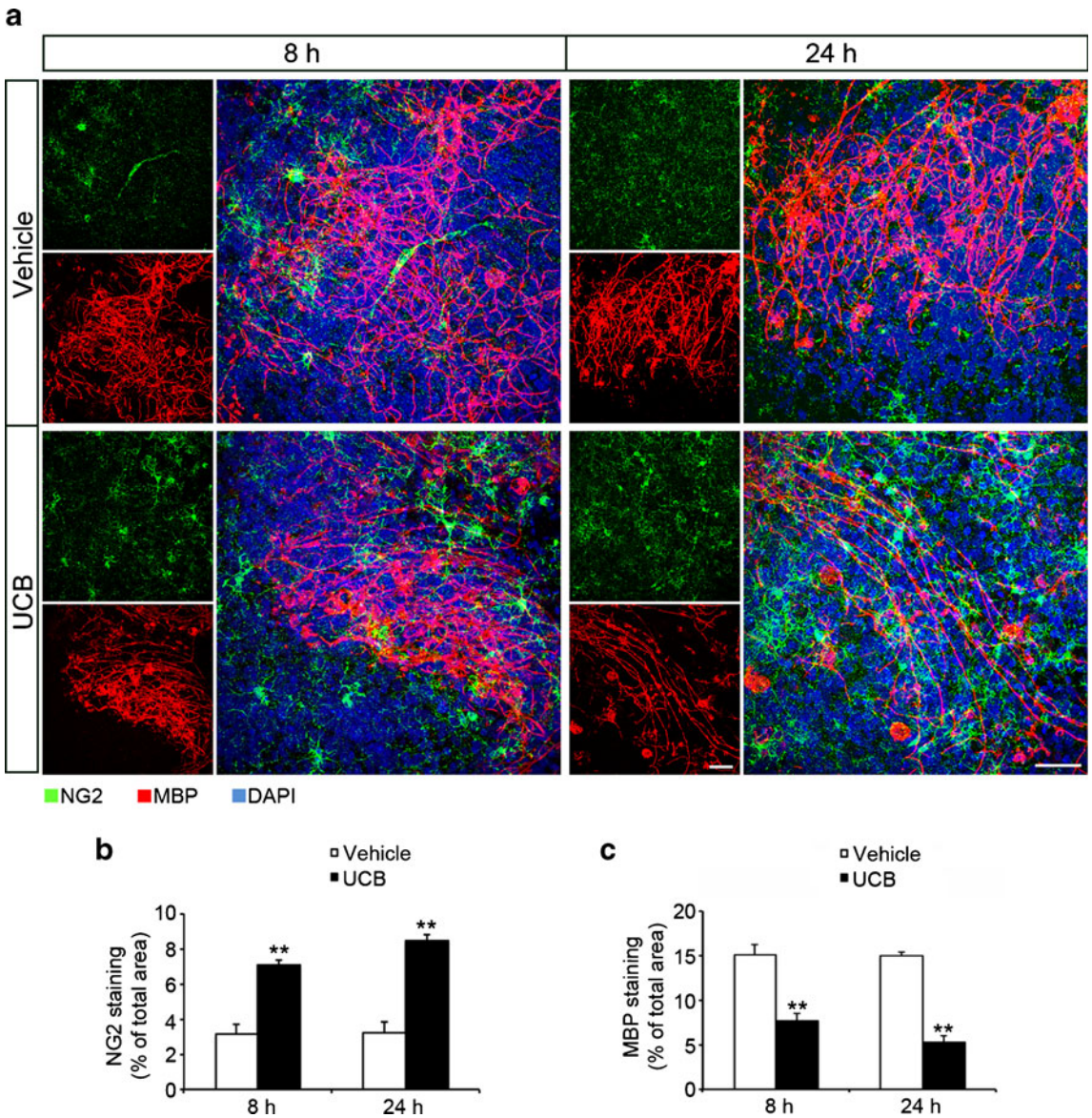

Fig. 3 Unconjugated bilirubin (*UCB*) arrests OL differentiation. Rat cerebellar slice cultures were exposed for 8 and 24 h to UCB, at 3 DIV, and maintained in culture until 7 DIV. **a** The cells were immunolabelled to identify OPC (NG2+ cells, *green*) and mature OL (myelin basic protein positive cells (*MBP*), *red*). Nuclei were counterstained with DAPI dye (*blue*). Representative images show an increase in the area occupied by NG2+ cells after 8 (*left column*) and 24 h (*right column*) UCB treatment. Area (percentage of total) occupied by NG2+ (**b**) and MBP staining cells (**c**) from sections of four distinct animals. Scale bar represents 50 μm. $^{**}P<0.01$ vs. respective vehicle

demonstrated that UCB impairs OL maturation in primary cultures of differentiating OL by reducing Olig1 and increasing Olig2 mRNA expression [23]. Once UCB increased the percentage of OPC in cerebellar slices, we investigated whether UCB treatment also affected Olig1 and Olig2 expression. Cerebellar slices were exposed to UCB as indicated before (Fig. 1a) and RNA isolated at 7 DIV to assess Olig1 and Olig2 mRNA expression (Fig. 4). Both acute and chronic treatments with UCB resulted in a reduction in Olig1 expression (0.76±0.05-fold for 8 h and 0.64±0.05-fold for 24 h, Bonferroni $P<0.01$) and in an increase in Olig2 mRNA expression (1.15±0.05-fold for 8 h, Bonferroni $P<0.05$ and 1.58±0.15-fold for 24 h, Bonferroni $P<0.01$) at 7 DIV, similarly to what we have previously observed.

UCB Triggers Reactive Gliosis in Rat Cerebellar Slice Cultures

Astrocytes and microglia can influence the formation of the myelin sheath [57]. Having observed in previous studies that UCB impairs myelinogenesis and promotes astroglial and microglial activation [12, 17], we wondered whether glial cells reactivity would account to the myelination defect produced by UCB in the cerebellar slices cultures. To do that, we treated them as before and immunostained at 7 DIV with antibodies recognising Iba-1 to identify microglia and GFAP to identify astrocytes. As shown in Fig. 5a, c, 8 and 24 h exposure to UCB induced microgliosis. The percentage of Iba-1+ cells per total area increased significant and was even more pronounced for the longer period of UCB exposure (1.59±0.15-fold for 8 h, Bonferroni $P<0.05$ and 1.74±0.24-fold for 24 h, Bonferroni $P<0.01$, ANOVA time of incubation F 8.75, $P<0.05$). In regard to astrocytes (Fig. 5b, d), we observed the same trend with a significant increased area occupied by GFAP+cells in cerebellar slices treated with UCB when compared with vehicle-treated ones (1.33±0.15-fold for 8 h, Bonferroni $P<0.05$ and 1.60±0.42-fold for 24 h, Bonferroni $P<0.01$). Altogether, these results clearly show that UCB exposure not only affects OL differentiation but also induces long lasting microgliosis and astrocytosis.

Treatment of Rat Cerebellar Slice Cultures with UCB Leads to a Fast and Transient Release of Glutamate

Glutamate has been demonstrated to be released from astrocytes, neurons and microglia upon UCB treatment and to be involved in UCB neurotoxicity [12, 13, 17]. In addition, glutamate is also known as a noxious molecule for OL during maturation and myelination [57]. Hence, we evaluated the accumulation of glutamate released into the culture media before UCB treatment, after UCB exposure for 8 or 24 h, and in the following days until 7 DIV (Fig. 1a). Glutamate release was fast, substantial and time dependent (Fig. 6). Both

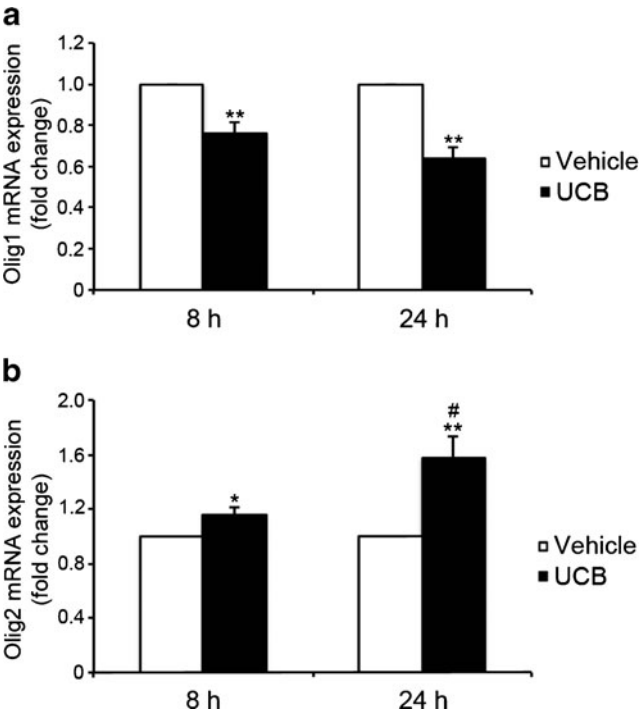

Fig. 4 Unconjugated bilirubin (*UCB*) induces a reduction of Olig1 and an increase of Olig2 mRNA expressions. Rat cerebellar slice cultures were exposed to UCB at 3 DIV for 8 and 24 h, and maintained in culture until 7 DIV. Relative levels of transcription factors Olig1 (**a**) and Olig2 (**b**) were determined by qRT-PCR with the $\Delta\Delta C_T$ method. Values are shown as mean±SEM from sections of five distinct animals, performed in triplicate and normalised to values of glyceraldehyde 3-phosphate dehydrogenase in the same samples. *$P<0.05$; **$P<0.01$ vs. vehicle; #$P<0.05$ vs. 8 h of UCB exposure

8- and 24 h-incubation periods with UCB doubled the secretion of glutamate into the culture medium (2.12±0.20-fold for 8 h and 2.78±0.41 for 24 h; Bonferroni $P<0.01$, ANOVA UCB treatment×time of incubation interaction F 6.18, $P<0.05$). The increase in glutamate, still noticeable at 5 DIV when the 24-h incubation was used (1.26±0.12-fold; Bonferroni $P<0.01$), returned to vehicle levels in the following days. This returned to basal levels suggests either a fast uptake

Fig. 5 Unconjugated bilirubin (*UCB*) induces microgliosis and ▶ astrocytosis. Rat cerebellar slice cultures were exposed to UCB at 3 DIV for 8 and 24 h and allowed to recover until 7 DIV. **a** OL were immunolabelled for myelin basic protein (*MBP*; *red*) and microglia for Iba-1 (*green*). Nuclei were counterstained with DAPI dye (*blue*). Representative images show an increase in the number of microglia after UCB treatment for 8 (*left column*) and 24 h (*right column*). **b** OL were immunolabelled as before and astrocytes were stained for glial fibrillary acidic protein (*GFAP*; *green*). Nuclei were counterstained with DAPI dye (*blue*). Representative images show an increase in the number of GFAP+ cells after UCB treatment for 8 (*left column*) and 24 h (*right column*). *Graph bars* represent the quantification of the area (percentage of total) occupied by Iba-1+- (**c**) and GFAP+-stained (**d**) cells after both times of incubation from sections of four distinct animals. *Scale bar* represents 50 μm. *$P<0.05$; **$P<0.01$ vs. respective vehicle

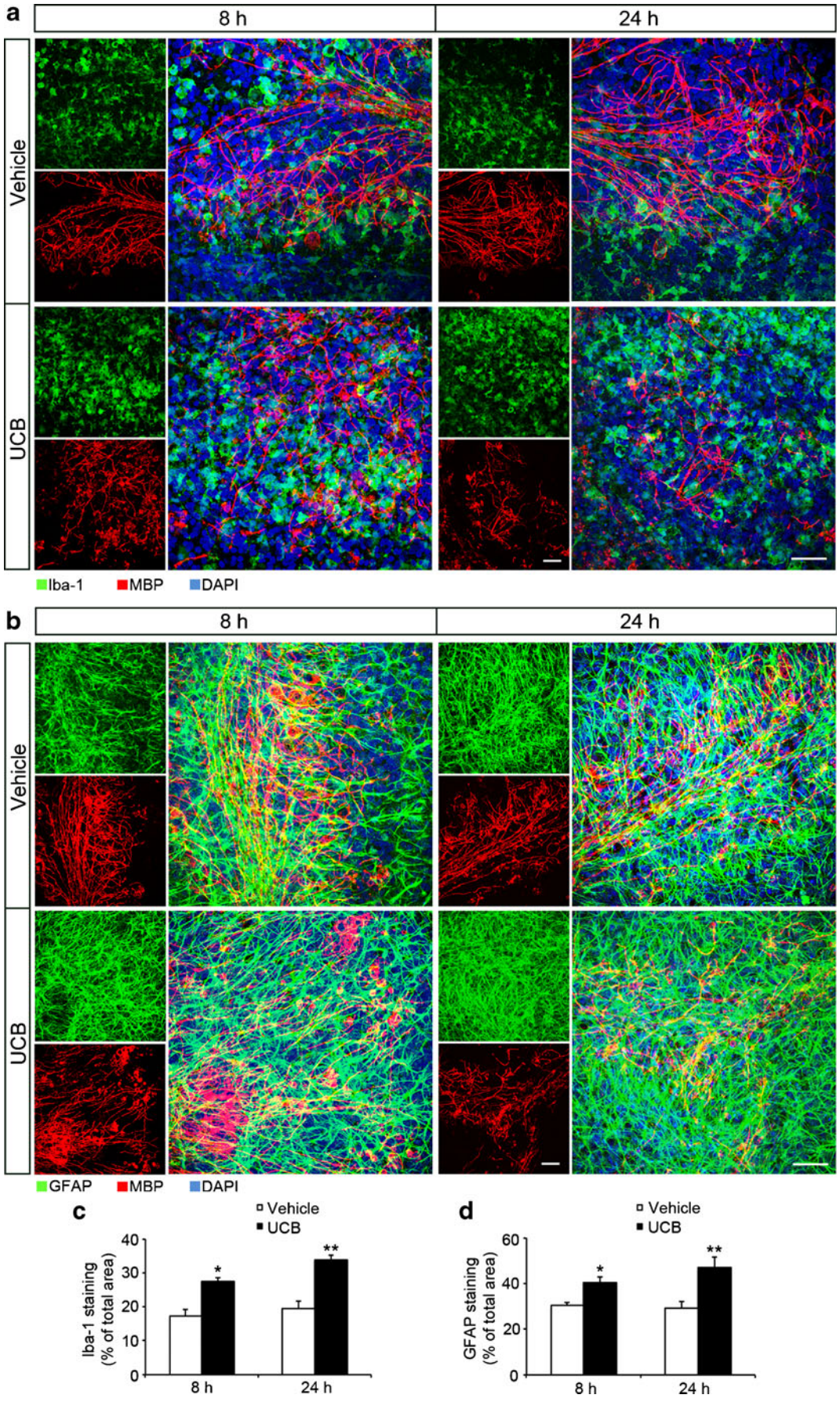
a
8 h
24 h
Vehicle
UCB
Iba-1
MBP
DAPI
b
8 h
24 h
Vehicle
UCB
GFAP
MBP
DAPI
c
Vehicle
UCB
Iba-1 staining (% of total area)
40
30
20
10
0
*
**
8 h
24 h
d
Vehicle
UCB
GFAP staining (% of total area)
60
40
20
0
*
**
8 h
24 h

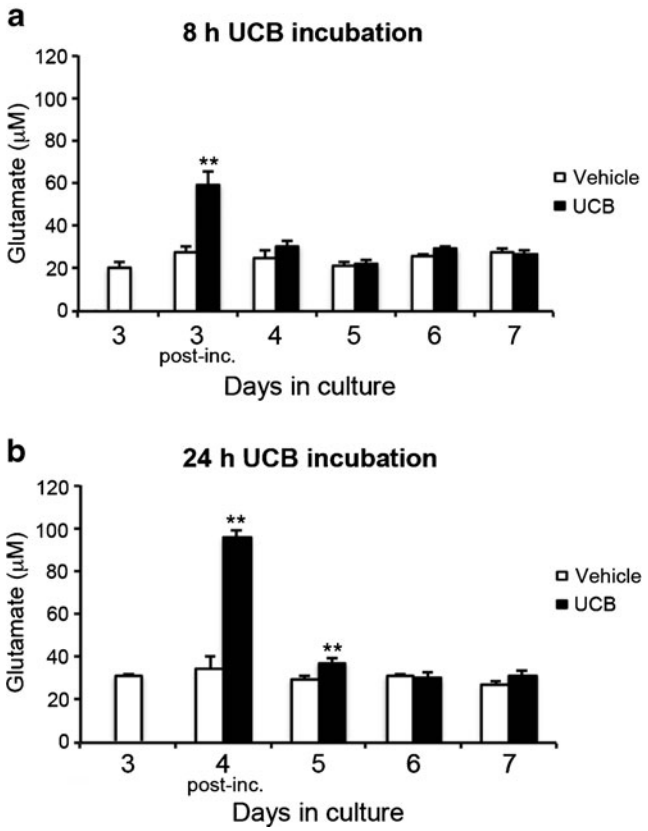

Fig. 6 Unconjugated bilirubin (*UCB*) induces glutamate release immediately after the treatment period. Rat cerebellar slice cultures were exposed to UCB at 3 DIV for 8 and 24 h and allowed to recover until 7 DIV. The samples for the glutamate quantification were collected from the culture medium exactly before and after UCB treatment, as well as in the following days till 7 DIV. *Graph bars* represent the glutamate content in the extracellular media after 8 (**a**) and 24 h (**b**) of exposure to UCB. Results are mean±SEM from at least five independent experiments performed in duplicate. $^{**}P<0.01$ vs. respective vehicle

and glutamate metabolism by glial cells or that its production directly depends from the presence of UCB in the culture.

UCB Stimulates the Secretion of TNF-α While Inhibiting the Release of IL-6 in Rat Cerebellar Slice Cultures

Supporting evidence indicates that UCB stimulates the production of pro-inflammatory cytokines by both astrocytes and microglia [12, 17]. Given that UCB triggered a marked gliosis in our present experimental model, we decided to characterise the temporal secretion of TNF-α, IL-1β, IL-6 and S100B into the incubation media. For that purpose, the cytokines released from cerebellar slices into the culture media were determined as we did for glutamate. As depicted in Fig. 7, cytokine production changed after the incubation with UCB and throughout the maintenance of the cerebellar slices in culture, including the vehicle-treated cultures. We hypothesise that this was due to the basal production of cytokines during the maintenance of slice cultures and their accumulation with time in culture since as half of the medium was replaced each day. After 8 h of incubation (Fig. 7a), UCB clearly induced a significant increase in TNF-α release (1.96±0.25-fold, Bonferroni $P<0.01$) that was maintained in the next 24 h (1.91±0.16-fold, Bonferroni $P<0.01$), slightly decreasing at 5 DIV, and increasing again at 6 and 7 DIV (2.55±0.96-fold, Bonferroni $P<0.05$ and 1.59±0.13-fold, Bonferroni $P<0.01$) respectively. As expected, 24 h exposure to UCB (Fig. 7b), produced a stronger secretion of TNF-α immediately after treatment (2.81±0.45-fold, Bonferroni $P<0.01$, ANOVA UCB treatmentxtime of incubation F 8.48, $P<0.01$) that peaked at 5 DIV (3.14±0.09-fold, Bonferroni $P<0.01$) and was maintained at 6 and 7 DIV (2.35±0.37- and 2.72±0.39-fold, respectively, Bonferroni $P<0.01$).

Regarding IL-6, we observed that the 8 h-treatment with UCB was not able to induce changes in the cytokine secretion (Fig. 7c). However, as depicted in Fig. 7d, 24 h exposure led to a significant decrease in IL-6 release immediately after UCB treatment (0.32±0.12-fold, Bonferroni $P<0.01$, ANOVA UCB treatment×time of incubation F 10.87, $P<0.01$) and 24 h later (0.38±0.20-fold, Bonferroni $P<0.05$). The basal levels were restored thereafter. This is not without precedent once similar UCB-induced inhibitory and transient effects on IL-6 secretion were previously observed in astrocytes [12].

Concerning IL-1β and S100B secretion, no noticeable changes occurred following UCB treatment when compared with vehicle-treated cultures (data not shown).

Neuronal Damage and Myelination Impairment by UCB Are Partially Mediated by Glutamate and TNF-α Toxicity

In a previous study, increased extracellular concentration of glutamate was toxic to OPC [38]. Although the mechanisms underlying TNF-α toxicity to the OL lineage remain unknown, a few reports show the deleterious effect of this cytokine in myelination [58]. Therefore, we investigated whether glutamate or TNF-α were involved in the myelination deficits caused by UCB in cerebellar slice cultures. Firstly, we added 10 μM of CNQX, an effective antagonist of AMPA receptors in OL [59], to the cerebellar slice culture media, which was maintained until 7 DIV (Fig. 1b). As shown in Fig. 8, CNQX was able to significantly enhance both the percentage of area occupied by neurofilaments (1.21±0.04-fold for 8 h and 1.23±0.06-fold for 24 h of UCB exposure, Bonferroni $P<0.05$) and the percentage of myelinated fibres (1.18±0.02-fold for 8 h, Bonferroni $P<0.05$ and 1.56±0.07-fold for 24 h, Bonferroni $P<0.01$, ANOVA UCB treatment×time of incubation F 55.29, $P<0.001$), suggesting that glutamate may play a role in UCB-induced delayed myelination. Next, cerebellar slice cultures were treated with a blocking anti-rat TNF-α antibody to neutralise the activity of this cytokine. The results obtained (Fig. 8) revealed that anti-rat TNF-α significantly enhanced the percentage of area occupied by neurofilaments (1.22±0.07-fold for 8 h, Bonferroni $P<0.05$ and 1.34±0.04-fold for 24 h, Bonferroni $P<0.01$), as well as the

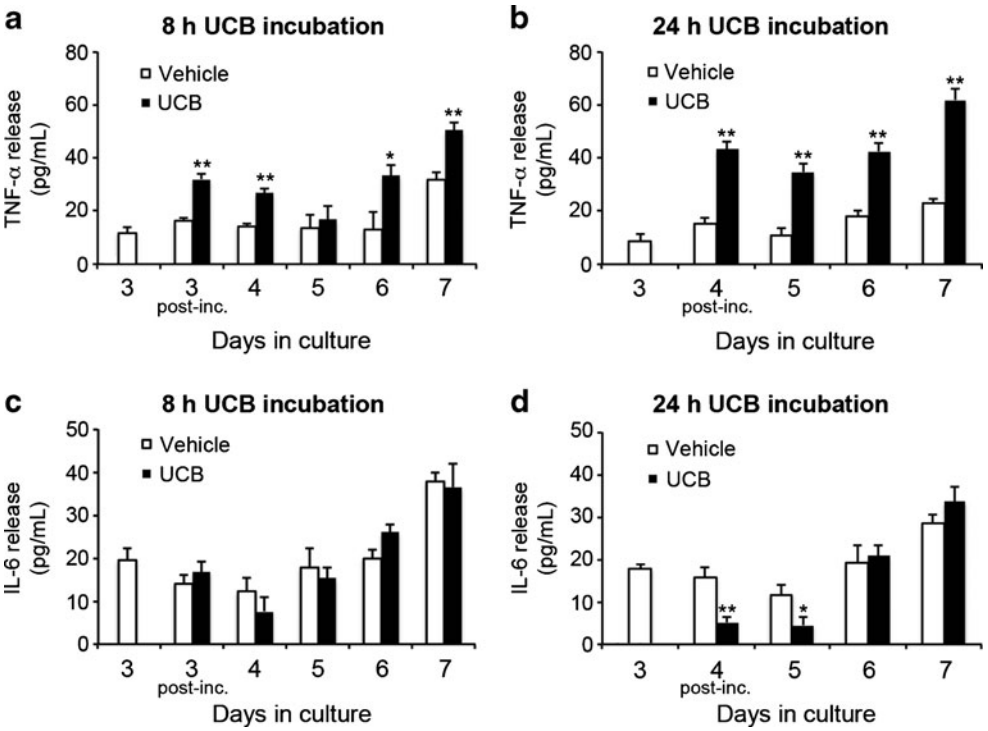

Fig. 7 Unconjugated bilirubin (*UCB*) leads to a sustained increase in TNF-α secretion and a transient decrease in IL-6 release. Rat cerebellar slice cultures were exposed to UCB at 3 DIV for 8 and 24 h and allowed to recover until 7 DIV. The samples for TNF-α and IL-6 determinations were collected from the culture medium exactly before and after UCB treatment, as well as in the following days till 7 DIV. *Graph bars* represent the TNF-α (**a**, **b**) and IL-6 (**c**, **d**) extracellular concentration after UCB treatment for 8 h (**a**, **c**) as well as for 24 h (**b**,**d**), respectively. Results are mean±SEM from at least five independent experiments performed in duplicate. *$P<0.05$; **$P<0.01$ vs. respective vehicle

percentage of myelinated fibres (1.28±0.01-fold for 8 h and 1.74±0.07-fold for 24 h, Bonferroni $P<0.01$, ANOVA UCB treatment×time of incubation F 55.29, $P<0.001$). These results demonstrated that TNF-α, even more effectively than glutamate, compromises myelination when rat cerebellar slice cultures are transiently exposed to UCB. Of note, treatment with the anti-TNF-α blocking antibody had no effect on glutamate release (data not shown), suggesting that both molecules may be acting by distinct pathways.

Discussion

We have shown that in our model of hyperbilirubinemia, UCB impairs myelination by inhibiting OPC differentiation and OL myelination. Accordingly, in cerebellar cultures treated with UCB, the percentage of OPC was higher than vehicle-treated slices and the percentage of mature and myelinating OL and myelinated fibres significantly lower than vehicle-treated slices. These defects were accompanied by gliosis, inflammation and excitotoxicity and were at least partially mediated by TNF-α and glutamate release to the extracellular medium.

Myelination occurs in the second week of postnatal development in rodents and in the last trimester of gestation in humans, but is only completed in some brain regions in early adulthood [60]. This tightly regulated process is closely coordinated between mature OL and neurons and is essential for normal information processing and learning. Disruption of WM is associated with a wide range of cognitive and psychiatric disorders [61] and WM abnormalities were observed in almost all infants with high levels of UCB examined at ages of 5 months or later [8]. Taking that into account, the identification of extrinsic and intrinsic factors modulating pathophysiological changes by UCB during neurodevelopment is crucial to understand developmental trajectories and to provide initial clues for preventive treatments. Our previous data, using dissociated OL cultures and myelinating axon-glia co-cultures demonstrated that UCB interferes with myelinogenesis [23]. However, these cultures have important limitations, as some relevant cell-cell interactions that occur only in the context of complex tissue cytoarchitecture are critical for deciphering the mechanisms of many normal and disease processes. Therefore, there is now increasing interest in the use of cerebellar organotypic slice cultures for studies on OL biology and myelination because of its retention of multi-cellular interactions and their easiness of manipulation [62, 63].

In this study, we started by evaluating if organotypic cerebellar slice cultures exposed to a solution of UCB mimicking the systemic bilirubin dynamics with a free UCB of 20 nM encountered in jaundiced newborns, evidenced changes in myelination and, if so, whether such effect was dependent on the duration of UCB exposure. We showed that although UCB treatment of cerebellar slices affected neuronal arborisation, myelination itself was clearly affected by UCB in a time-dependent manner. These effects were observed at 7 DIV, at least 4 days after UCB treatment, indicating that cerebellar slices did not recover from UCB toxic effect. Similar to what

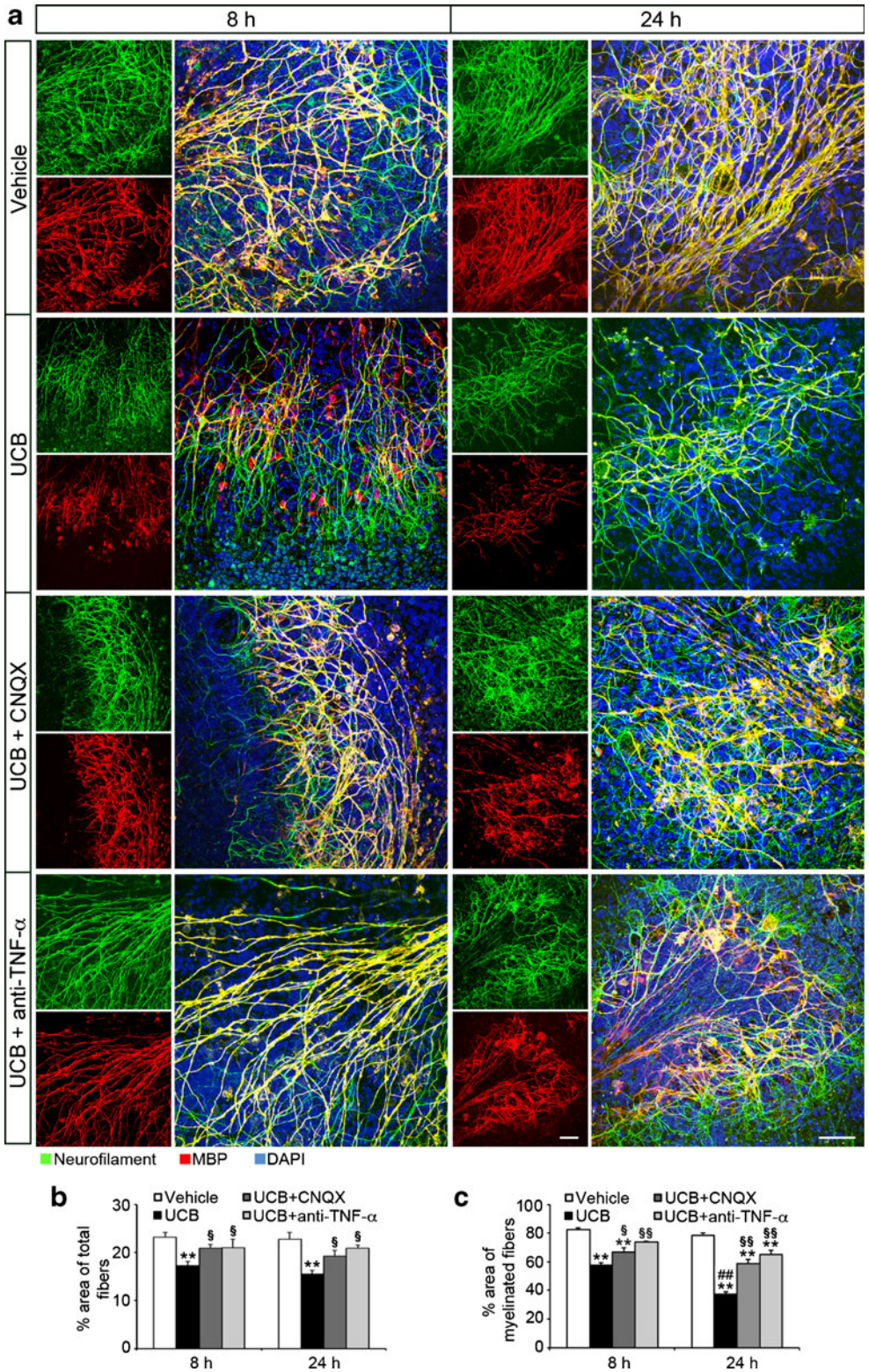

Fig. 8 Impairment in neuronal fibre number and in myelination by unconjugated bilirubin (*UCB*) is prevented by AMPA and TNF-α inhibitors. Rat cerebellar slice cultures were exposed to UCB at 3 DIV for 8 and 24 h and maintained in culture until 7 DIV. In parallel experiments, slices were incubated with 10 μM 6-cyano-7-nitroquinoxaline-2,3-dione (*CNQX*), a competitive antagonist of AMPA glutamate receptor or with 0.15 μg/mL anti-rat TNF-α. **a** OL were immunolabelled for myelin basic protein (*MBP*; *red*) to detect myelinated tracts and neurofilaments (*NF*; *green*) to detect neuronal axons. Nuclei were counterstained with DAPI dye (*blue*). Representative images show increased number of total fibres and of myelinated fibres after 8 (*left column*) or 24 h (*right column*) incubation periods with AMPA and TNF-α inhibitors. *Graph bars* represent the percentage of total area occupied by neurofilaments (**b**) and the percentage of the area occupied by myelinated fibres (**c**) from sections of four distinct animals. *Scale bar* represents 50 μm. $^{**}P<0.01$ vs. respective vehicle; $^{\#\#}P<0.01$ vs. 8 h of UCB exposure; $^{\S}P<0.05$; $^{\S\S}P<0.01$ vs. respective UCB

we observed earlier in our in vitro myelination model [23], we also found that exposure to UCB reduced the percentage of MBP+OL and, as a result, increased the percentage of NG2+ OPC, showing that UCB inhibits OPC differentiation. As previously shown, the myelination effect is highly dependent on the extent of UCB interaction with the cells, justifying the risk indicated for the duration of hyperbilirubinemia in the emergence of neurologic deficits [64].

Similarly to what we have observed with UCB, a recent study using an organotypic slice culture model of chronic WM injury [65] has demonstrated that myelination failure involves a reduction in the number of differentiated OL, and that inhibition of OPC differentiation results in excessive proliferation and accumulation of OPC. These in vitro and ex vivo responses are similar to those described in neonatal rodents following hypoxia/ischemia and intermittent hypoxia mimicking apnea of prematurity, where the failure of preoligodendrocytes to maturate led to myelination deficits [66, 67]. This kind of association was additionally demonstrated in preterm fetal sheep, following hypoxia/ischemia [68], and in preterm autopsy human cases presenting diffuse WM injury [69]. Consequently, the arrest of OL maturation may expand the developmental window of WM immaturity, which may enhance the risk of brain injuries during neonatal jaundice.

Over the last few years, valuable insights have been made in the transcriptional program necessary for the differentiation of OPC into mature myelinating OL [57]. In particular, the functions of the transcription factors Olig1 and Olig2 in defining and regulating the maturation of the oligodendroglial lineage [70]. Although Olig1 regulates myelin gene expression, Olig2 is implicated in the specification of OPC during development [33, 35]. In agreement with our data in differentiating cultures of primary OL [23], here we evidenced that exposure to UCB determines an increase in Olig2 mRNA expression, but a reduction in that of Olig1. This finding is in line with studies demonstrating that Olig1 expression is essential for MBP, proteolipid protein and myelin associated glycoprotein transcription, whereas that of Olig2 is detected in freshly isolated OPC, but is not involved in either process outgrowth, or myelination and myelin membrane maintenance [34, 71].

In addition to their vital role in the homeostatic regulation of the developing and adult brain, astrocytes and microglia also play critical roles following CNS damage [72]. Therefore, we analysed how these cells responded to UCB exposure in cerebellar slice cultures. We observed a significant increase in the percentage of area occupied by astrocytes and microglia after UCB exposure when compared with vehicle-treated slices. In this context, astroglial reactivity was identified in ischemia [73], trauma [74] and infection [75]. Most strikingly, a recent study performed in an organotypic slice culture model of chronic WM injury has demonstrated a rapid and progressive reactive astrocytosis and microglia accumulation in the WM [65]. Prenatal ischemia in rats with WM injury was also shown to lead to astrogliosis in several brain regions, such as the hippocampus and cortex [76, 77]. Additionally, microglial activation was observed during neuro-inflammatory events related to the pathogenesis of early periventricular leukomalacia [78] and both microgliosis and astrogliosis were noticed during WM injury in premature infants [69].

In response to injury, both astrocytes and microglia turn into an activated state that entails release of pro-inflammatory cytokines, oxygen radicals and proteases [79, 80]. In line with an increase in astrocyte and microglia cell number, we show that after UCB exposure there is an accumulation of TNF-α in the culture medium. Interestingly, the amount of this cytokine directly increases with the time of incubation indicating sustained activation of cells by UCB, even after its removal from the culture medium. Release of TNF-α was reported to occur in traumatic brain injury [81] and demonstrated by us after UCB-treatment of pure cultures of microglia and astrocytes using our model of experimental neonatal jaundice [12, 17]. By contrast, 24 h of exposure to UCB significantly inhibits IL-6 secretion, similar to what we obtained for a short incubation of astrocytes with UCB [12, 16]. Interestingly, we have shown that UCB mostly induces TNF-α release from astrocytes [16], and IL-1β from microglia [82]. Thus, we speculate that in our cerebellar slice cultures astrocytes were the main producers of TNF-α and that microglia assumed a more neuroprotective phenotype. Increased production of TNF-α may cause disruption of WM maturation and injury, as demonstrated by the impairment of myelination in spinal cord-derived cultures [83] and by hypomyelination in periventricular leukomalacia in the presence of high levels of this cytokine [84, 85]. In fact, TNF-α is known to damage OL [86], resulting in deficits in myelin production. Our results following neutralisation of TNF-α with a blocking antibody emphasise TNF-α contribution to the overall loss of neuronal fibres and their myelination.

Moreover, glutamate excitotoxicity has been shown to cause damage to the developing brain in animal models of trauma [87], as well as in hypoxia/ischemia [88], and overactivation of non-NMDA glutamate receptors evidenced to impair OPC proliferation and OL development [89, 90]. The increased glutamate efflux in our model is in line with previous data indicating that UCB interferes with glutamate uptake into synaptic vesicles [91], astrocytes and neurons [10, 92], although it may also increase glutamate release from neurons and glia [12, 13, 17]. In addition, AMPA receptors in WM glia are suggested to play a role in the delayed posttraumatic spinal cord WM degeneration [93], whereas the AMPA receptor antagonist NBQX showed to attenuate hypoxia/ischemia-mediated OL death in subcortical WM [94]. Therefore, by using the AMPA receptor antagonist CNQX, we show that the release of glutamate can mediate the UCB deleterious effects on myelination.

Collectively, our results reinforce and expand the conclusions of our previous work using dissociated cultures revealing

that UCB impairs myelination and show, for the first time, that moderately elevated levels of UCB inhibit OL differentiation and increase gliosis in the complex multicellular environment of the three-dimensional structure of the cerebellar slice cultures.

Altogether, our data suggest that the reduced myelination observed in some infants with bilirubin encephalopathy [8, 30] can derive from OL maturation arrest, resulting in impaired myelination during the perinatal period. Our data also indicate that UCB-induced changes in OL development may be related with alterations in the transcriptional program of OL, as well as with accumulation of TNF-α and glutamate in the extracellular medium. As our studies were performed with levels of unbound bilirubin that mimic situations of clinical neonatal jaundice, we propose that hyperbilirubinemia may trigger defective myelination and gliosis causing inflammatory and excitotoxic responses, which are important features that deserve to be considered in neuroprotective strategies for the treatment of BIND.

Acknowledgements This work was supported by FEDER (COMPETE Programme) and by National funds (Fundação para a Ciência e a Tecnologia (FCT) project PTDC/SAU-NEU/64385/2006 to D.B. and project PEst-OE/SAU/UI4013/2011 and 2012). A. B. was recipient of a Ph.D. fellowship (SFRH/BD/43885/2008) from FCT. H.S.D. is supported by a Marie Curie Intra European Fellowship within the 7th European Community Framework Programme. Work in the lab of J.B.R. was supported by a PTDC/BIA-BCM/112730/2009 from FCT. The funding organisation had no role in study design, data collection and analysis, decision to publish or preparation of the manuscript.

References

1. Cohen RS, Wong RJ, Stevenson DK (2010) Understanding neonatal jaundice: a perspective on causation. Pediatr Neonatol 51(3):143–148. doi:10.1016/S1875-9572(10)60027-7
2. Kaplan M, Muraca M, Hammerman C, Rubaltelli FF, Vilei MT, Vreman HJ, Stevenson DK (2002) Imbalance between production and conjugation of bilirubin: a fundamental concept in the mechanism of neonatal jaundice. Pediatrics 110(4):e47
3. Bratlid D (1990) How bilirubin gets into the brain. Clin Perinatol 17(2):449–465
4. Brites D (2012) The evolving landscape of neurotoxicity by unconjugated bilirubin: role of glial cells and inflammation. Front Pharmacol 3:88. doi:10.3389/fphar.2012.00088
5. Hansen TW (2000) Pioneers in the scientific study of neonatal jaundice and kernicterus. Pediatrics 106(2):E15
6. Ahdab-Barmada M, Moossy J (1984) The neuropathology of kernicterus in the premature neonate: diagnostic problems. J Neuropathol Exp Neurol 43(1):45–56
7. Brito MA, Zurolo E, Pereira P, Barroso C, Aronica E, Brites D (2011) Cerebellar axon/myelin loss, angiogenic sprouting, and neuronal increase of vascular endothelial growth factor in a preterm infant with kernicterus. J Child Neurol. doi:10.1177/0883073811423975
8. Gkoltsiou K, Tzoufi M, Counsell S, Rutherford M, Cowan F (2008) Serial brain MRI and ultrasound findings: relation to gestational age, bilirubin level, neonatal neurologic status and neurodevelopmental outcome in infants at risk of kernicterus. Early Hum Dev 84(12):829–838. doi:10.1016/j.earlhumdev.2008.09.008
9. Hanko E, Hansen TW, Almaas R, Paulsen R, Rootwelt T (2006) Synergistic protection of a general caspase inhibitor and MK-801 in bilirubin-induced cell death in human NT2-N neurons. Pediatr Res 59(1):72–77. doi:10.1203/01.pdr.0000191135.63586.08
10. Silva RF, Rodrigues CM, Brites D (2002) Rat cultured neuronal and glial cells respond differently to toxicity of unconjugated bilirubin. Pediatr Res 51(4):535–541
11. Brites DaB, A (2012) Bilirubin toxicity. In: Stevenson DK MM, Watchko JF (ed) Care of the jaundiced neonate. McGraw-Hill, New York, pp 115–143
12. Fernandes A, Silva RF, Falcao AS, Brito MA, Brites D (2004) Cytokine production, glutamate release and cell death in rat cultured astrocytes treated with unconjugated bilirubin and LPS. J Neuroimmunol 153(1–2):64–75. doi:10.1016/j.jneuroim.2004.04.007
13. Falcao AS, Fernandes A, Brito MA, Silva RF, Brites D (2006) Bilirubin-induced immunostimulant effects and toxicity vary with neural cell type and maturation state. Acta Neuropathol 112(1):95–105. doi:10.1007/s00401-006-0078-4
14. Hanko E, Hansen TW, Almaas R, Rootwelt T (2006) Recovery after short-term bilirubin exposure in human NT2-N neurons. Brain Res 1103(1):56–64. doi:10.1016/j.brainres.2006.05.083
15. Brito MA, Vaz AR, Silva SL, Falcao AS, Fernandes A, Silva RF, Brites D (2010) N-methyl-aspartate receptor and neuronal nitric oxide synthase activation mediate bilirubin-induced neurotoxicity. Mol Med 16(9–10):372–380. doi:10.2119/molmed.2009.00152
16. Fernandes A, Falcao AS, Silva RF, Gordo AC, Gama MJ, Brito MA, Brites D (2006) Inflammatory signalling pathways involved in astroglial activation by unconjugated bilirubin. J Neurochem 96(6):1667–1679. doi:10.1111/j.1471-4159.2006.03680.x
17. Gordo AC, Falcao AS, Fernandes A, Brito MA, Silva RF, Brites D (2006) Unconjugated bilirubin activates and damages microglia. J Neurosci Res 84(1):194–201. doi:10.1002/jnr.20857
18. Silva SL, Osorio C, Vaz AR, Barateiro A, Falcao AS, Silva RF, Brites D (2011) Dynamics of neuron-glia interplay upon exposure to unconjugated bilirubin. J Neurochem 117(3):412–424. doi:10.1111/j.1471-4159.2011.07200.x
19. Chang FY, Lee CC, Huang CC, Hsu KS (2009) Unconjugated bilirubin exposure impairs hippocampal long-term synaptic plasticity. PLoS One 4(6):e5876. doi:10.1371/journal.pone.0005876
20. Shapiro SM (2005) Definition of the clinical spectrum of kernicterus and bilirubin-induced neurologic dysfunction (BIND). J Perinatol 25(1):54–59. doi:10.1038/sj.jp.7211157
21. Fernandes A, Falcao AS, Abranches E, Bekman E, Henrique D, Lanier LM, Brites D (2009) Bilirubin as a determinant for altered neurogenesis, neuritogenesis, and synaptogenesis. Developmental neurobiology 69(9):568–582. doi:10.1002/dneu.20727
22. Barateiro A, Vaz AR, Silva SL, Fernandes A, Brites D (2012) ER Stress, Mitochondrial dysfunction and calpain/JNK Activation are involved in oligodendrocyte precursor cell death by unconjugated bilirubin. Neuromolecular Med 14(4):285–302. doi:10.1007/s12017-012-8187-9
23. Barateiro A, Miron VE, Santos SD, Relvas JB, Fernandes A, Ffrench-Constant C, Brites D (2013) Unconjugated bilirubin restricts oligodendrocyte differentiation and axonal myelination. Mol Neurobiol 47(2):632–644. doi:10.1007/s12035-012-8364-8
24. Castonguay A, Levesque S, Robitaille R (2001) Glial cells as active partners in synaptic functions. Prog Brain Res 132:227–240. doi:10.1016/S0079-6123(01)32079-4
25. Volterra A, Meldolesi J (2005) Astrocytes, from brain glue to communication elements: the revolution continues. Nat Rev Neurosci 6(8):626–640. doi:10.1038/nrn1722
26. Lai AY, Todd KG (2008) Differential regulation of trophic and proinflammatory microglial effectors is dependent on severity of neuronal injury. Glia 56(3):259–270. doi:10.1002/glia.20610

27. Ghoumari AM, Ibanez C, El-Etr M, Leclerc P, Eychenne B, O'Malley BW, Baulieu EE, Schumacher M (2003) Progesterone and its metabolites increase myelin basic protein expression in organotypic slice cultures of rat cerebellum. J Neurochem 86(4):848–859
28. Kasparov S, Teschemacher AG, Paton JF (2002) Dynamic confocal imaging in acute brain slices and organotypic slice cultures using a spectral confocal microscope with single photon excitation. Exp Physiol 87(6):715–724
29. Bhutani VK, Stevenson DK (2011) The need for technologies to prevent bilirubin-induced neurologic dysfunction syndrome. Semin Perinatol 35(3):97–100. doi:10.1053/j.semperi.2011.02.002
30. Brito MA, Zurolo E, Pereira P, Barroso C, Aronica E, Brites D (2012) Cerebellar axon/myelin loss, angiogenic sprouting, and neuronal increase of vascular endothelial growth factor in a preterm infant with kernicterus. J Child Neurol 27(5):615–624. doi:10.1177/0883073811423975
31. Zhang H, Jarjour AA, Boyd A, Williams A (2011) Central nervous system remyelination in culture—a tool for multiple sclerosis research. Exp Neurol 230(1):138–148. doi:10.1016/j.expneurol.2011.04.009
32. Craig A, Ling Luo N, Beardsley DJ, Wingate-Pearse N, Walker DW, Hohimer AR, Back SA (2003) Quantitative analysis of perinatal rodent oligodendrocyte lineage progression and its correlation with human. Exp Neurol 181(2):231–240
33. Lu QR, Sun T, Zhu Z, Ma N, Garcia M, Stiles CD, Rowitch DH (2002) Common developmental requirement for Olig function indicates a motor neuron/oligodendrocyte connection. Cell 109(1):75–86
34. Xin M, Yue T, Ma Z, Wu FF, Gow A, Lu QR (2005) Myelinogenesis and axonal recognition by oligodendrocytes in brain are uncoupled in Olig1-null mice. J Neurosci 25(6):1354–1365. doi:10.1523/JNEUROSCI.3034-04.2005
35. Copray S, Balasubramaniyan V, Levenga J, de Bruijn J, Liem R, Boddeke E (2006) Olig2 overexpression induces the in vitro differentiation of neural stem cells into mature oligodendrocytes. Stem Cells 24(4):1001–1010. doi:10.1634/stemcells.2005-0239
36. Buchet D, Baron-Van Evercooren A (2009) In search of human oligodendroglia for myelin repair. Neurosci Lett 456(3):112–119. doi:10.1016/j.neulet.2008.09.086
37. Nave KA (2010) Myelination and the trophic support of long axons. Nat Rev Neurosci 11(4):275–283. doi:10.1038/nrn2797
38. Deng W, Rosenberg PA, Volpe JJ, Jensen FE (2003) Calcium-permeable AMPA/kainate receptors mediate toxicity and preconditioning by oxygen-glucose deprivation in oligodendrocyte precursors. Proc Natl Acad Sci U S A 100(11):6801–6806. doi:10.1073/pnas.1136624100
39. Itoh T, Beesley J, Itoh A, Cohen AS, Kavanaugh B, Coulter DA, Grinspan JB, Pleasure D (2002) AMPA glutamate receptor-mediated calcium signaling is transiently enhanced during development of oligodendrocytes. J Neurochem 81(2):390–402
40. Rosenberg PA, Dai W, Gan XD, Ali S, Fu J, Back SA, Sanchez RM, Segal MM, Follett PL, Jensen FE, Volpe JJ (2003) Mature myelin basic protein-expressing oligodendrocytes are insensitive to kainate toxicity. J Neurosci Res 71(2):237–245. doi:10.1002/jnr.10472
41. Li S, Stys PK (2000) Mechanisms of ionotropic glutamate receptor-mediated excitotoxicity in isolated spinal cord white matter. J Neurosci 20(3):1190–1198
42. De Biase LM, Kang SH, Baxi EG, Fukaya M, Pucak ML, Mishina M, Calabresi PA, Bergles DE (2011) NMDA receptor signaling in oligodendrocyte progenitors is not required for oligodendrogenesis and myelination. J Neurosci 31(35):12650–12662. doi:10.1523/JNEUROSCI.2455-11.2011
43. McDonagh AF, Assisi F (1972) The ready isomerization of bilirubin IX- in aqueous solution. Biochem J 129(3):797–800
44. Silva SL, Vaz AR, Diogenes MJ, van Rooijen N, Sebastiao AM, Fernandes A, Silva RF, Brites D (2012) Neuritic growth impairment and cell death by unconjugated bilirubin is mediated by NO and glutamate, modulated by microglia, and prevented by glycoursodeoxycholic acid and interleukin-10. Neuropharmacology 62(7):2398–2408. doi:10.1016/j.neuropharm.2012.02.002
45. Ostrow JD, Pascolo L, Shapiro SM, Tiribelli C (2003) New concepts in bilirubin encephalopathy. Eur J Clin Invest 33(11):988–997
46. Ostrow JD, Pascolo L, Tiribelli C (2003) Reassessment of the unbound concentrations of unconjugated bilirubin in relation to neurotoxicity in vitro. Pediatric research 54(6):926
47. Brito MA, Silva RF, Brites D (2002) Bilirubin induces loss of membrane lipids and exposure of phosphatidylserine in human erythrocytes. Cell Biol Toxicol 18(3):181–192
48. Brito MA, Brondino CD, Moura JJ, Brites D (2001) Effects of bilirubin molecular species on membrane dynamic properties of human erythrocyte membranes: a spin label electron paramagnetic resonance spectroscopy study. Arch Biochem Biophys 387(1):57–65. doi:10.1006/abbi.2000.2210
49. Ahlfors CE, Wennberg RP, Ostrow JD, Tiribelli C (2009) Unbound (free) bilirubin: improving the paradigm for evaluating neonatal jaundice. Clin Chem 55(7):1288–1299. doi:10.1373/clinchem.2008.121269
50. Palmela I, Sasaki H, Cardoso FL, Moutinho M, Kim KS, Brites D, Brito MA (2012) Time-dependent dual effects of high levels of unconjugated bilirubin on the human blood–brain barrier lining. Front Cell Neurosci 6:22. doi:10.3389/fncel.2012.00022
51. Labombarda F, Gonzalez SL, Lima A, Roig P, Guennoun R, Schumacher M, de Nicola AF (2009) Effects of progesterone on oligodendrocyte progenitors, oligodendrocyte transcription factors, and myelin proteins following spinal cord injury. Glia 57(8):884–897. doi:10.1002/glia.20814
52. Falcao AS, Silva RF, Vaz AR, Silva SL, Fernandes A, Brites D (2013) Cross-talk between neurons and astrocytes in response to bilirubin: early beneficial effects. Neurochem Res 38(3):644–659. doi:10.1007/s11064-012-0963-2
53. Lu QR, Yuk D, Alberta JA, Zhu Z, Pawlitzky I, Chan J, McMahon AP, Stiles CD, Rowitch DH (2000) Sonic hedgehog–regulated oligodendrocyte lineage genes encoding bHLH proteins in the mammalian central nervous system. Neuron 25(2):317–329
54. Zhou Q, Anderson DJ (2002) The bHLH transcription factors OLIG2 and OLIG1 couple neuronal and glial subtype specification. Cell 109(1):61–73
55. Dugas JC, Tai YC, Speed TP, Ngai J, Barres BA (2006) Functional genomic analysis of oligodendrocyte differentiation. J Neurosci 26(43):10967–10983. doi:10.1523/JNEUROSCI.2572-06.2006
56. Nicolay DJ, Doucette JR, Nazarali AJ (2007) Transcriptional control of oligodendrogenesis. Glia 55(13):1287–1299. doi:10.1002/glia.20540
57. Emery B (2010) Regulation of oligodendrocyte differentiation and myelination. Science 330(6005):779–782. doi:10.1126/science.1190927
58. Jenkins HG, Ikeda H (1992) Tumour necrosis factor causes an increase in axonal transport of protein and demyelination in the mouse optic nerve. J Neurol Sci 108(1):99–104
59. Chen H, Kintner DB, Jones M, Matsuda T, Baba A, Kiedrowski L, Sun D (2007) AMPA-mediated excitotoxicity in oligodendrocytes: role for Na(+)-K(+)-Cl(−) co-transport and reversal of Na(+)/Ca(2+) exchanger. J Neurochem 102(6):1783–1795. doi:10.1111/j.1471-4159.2007.04638.x
60. Rice D, Barone S Jr (2000) Critical periods of vulnerability for the developing nervous system: evidence from humans and animal models. Environ Health Perspect 108(Suppl 3):511–533
61. Fields RD (2008) White matter in learning, cognition and psychiatric disorders. Trends Neurosci 31(7):361–370. doi:10.1016/j.tins.2008.04.001
62. Yang Y, Lewis R, Miller RH (2011) Interactions between oligodendrocyte precursors control the onset of CNS myelination. Dev Biol 350(1):127–138. doi:10.1016/j.ydbio.2010.11.028
63. Gadea A, Aguirre A, Haydar TF, Gallo V (2009) Endothelin-1 regulates oligodendrocyte development. The Journal of neuroscience

: the official journal of the Society for Neuroscience 29(32):10047–10062. doi:10.1523/JNEUROSCI.0822-09.2009
64. Johnson L, Bhutani VK (2011) The clinical syndrome of bilirubin-induced neurologic dysfunction. Semin Perinatol 35(3):101–113. doi:10.1053/j.semperi.2011.02.003
65. Dean JM, Riddle A, Maire J, Hansen KD, Preston M, Barnes AP, Sherman LS, Back SA (2011) An organotypic slice culture model of chronic white matter injury with maturation arrest of oligodendrocyte progenitors. Mol Neurodegener 6:46. doi:10.1186/1750-1326-6-46
66. Segovia KN, McClure M, Moravec M, Luo NL, Wan Y, Gong X, Riddle A, Craig A, Struve J, Sherman LS, Back SA (2008) Arrested oligodendrocyte lineage maturation in chronic perinatal white matter injury. Ann Neurol 63(4):520–530. doi:10.1002/ana.21359
67. Cai J, Tuong CM, Zhang Y, Shields CB, Guo G, Fu H, Gozal D (2012) Mouse intermittent hypoxia mimicking apnoea of prematurity: effects on myelinogenesis and axonal maturation. J Pathol 226(3):495–508. doi:10.1002/path.2980
68. Riddle A, Dean J, Buser JR, Gong X, Maire J, Chen K, Ahmad T, Cai V, Nguyen T, Kroenke CD, Hohimer AR, Back SA (2011) Histopathological correlates of magnetic resonance imaging-defined chronic perinatal white matter injury. Ann Neurol 70(3):493–507. doi:10.1002/ana.22501
69. Buser JR, Maire J, Riddle A, Gong X, Nguyen T, Nelson K, Luo NL, Ren J, Struve J, Sherman LS, Miller SP, Chau V, Hendson G, Ballabh P, Grafe MR, Back SA (2012) Arrested preoligodendrocyte maturation contributes to myelination failure in premature infants. Ann Neurol 71(1):93–109. doi:10.1002/ana.22627
70. Ligon KL, Fancy SP, Franklin RJ, Rowitch DH (2006) Olig gene function in CNS development and disease. Glia 54(1):1–10. doi:10.1002/glia.20273
71. Niu J, Mei F, Wang L, Liu S, Tian Y, Mo W, Li H, Lu QR, Xiao L (2012) Phosphorylated olig1 localizes to the cytosol of oligodendrocytes and promotes membrane expansion and maturation. Glia. doi:10.1002/glia.22364
72. Liu W, Tang Y, Feng J (2011) Cross talk between activation of microglia and astrocytes in pathological conditions in the central nervous system. Life Sci 89(5–6):141–146. doi:10.1016/j.lfs.2011.05.011
73. Biran V, Joly LM, Heron A, Vernet A, Vega C, Mariani J, Renolleau S, Charriaut-Marlangue C (2006) Glial activation in white matter following ischemia in the neonatal P7 rat brain. Exp Neurol 199(1):103–112. doi:10.1016/j.expneurol.2006.01.037
74. Rostworowski M, Balasingam V, Chabot S, Owens T, Yong VW (1997) Astrogliosis in the neonatal and adult murine brain post-trauma: elevation of inflammatory cytokines and the lack of requirement for endogenous interferon-gamma. J Neurosci 17(10):3664–3674
75. Rousset CI, Chalon S, Cantagrel S, Bodard S, Andres C, Gressens P, Saliba E (2006) Maternal exposure to LPS induces hypomyelination in the internal capsule and programmed cell death in the deep gray matter in newborn rats. Pediatr Res 59(3):428–433. doi:10.1203/01.pdr.0000199905.08848.55
76. Delcour M, Russier M, Amin M, Baud O, Paban V, Barbe MF, Coq JO (2012) Impact of prenatal ischemia on behavior, cognitive abilities and neuroanatomy in adult rats with white matter damage. Behav Brain Res 232(1):233–244. doi:10.1016/j.bbr.2012.03.029
77. Delcour M, Russier M, Xin DL, Massicotte VS, Barbe MF, Coq JO (2011) Mild musculoskeletal and locomotor alterations in adult rats with white matter injury following prenatal ischemia. Int J Dev Neurosci 29(6):593–607. doi:10.1016/j.ijdevneu.2011.02.010
78. Haynes RL, Folkerth RD, Trachtenberg FL, Volpe JJ, Kinney HC (2009) Nitrosative stress and inducible nitric oxide synthase expression in periventricular leukomalacia. Acta Neuropathol 118(3):391–399. doi:10.1007/s00401-009-0540-1
79. Kim SU, de Vellis J (2005) Microglia in health and disease. J Neurosci Res 81(3):302–313. doi:10.1002/jnr.20562
80. Allan SM, Rothwell NJ (2001) Cytokines and acute neurodegeneration. Nat Rev Neurosci 2(10):734–744. doi:10.1038/35094583
81. Bermpohl D, You Z, Lo EH, Kim HH, Whalen MJ (2007) TNF alpha and Fas mediate tissue damage and functional outcome after traumatic brain injury in mice. J Cereb Blood Flow Metab 27(11):1806–1818. doi:10.1038/sj.jcbfm.9600487
82. Silva SL, Vaz AR, Barateiro A, Falcao AS, Fernandes A, Brito MA, Silva RF, Brites D (2010) Features of bilirubin-induced reactive microglia: from phagocytosis to inflammation. Neurobiol Dis 40(3):663–675. doi:10.1016/j.nbd.2010.08.010
83. Pang Y, Zheng B, Kimberly SL, Cai Z, Rhodes PG, Lin RC (2012) Neuron-oligodendrocyte myelination co-culture derived from embryonic rat spinal cord and cerebral cortex. Brain Behav 2(1):53–67. doi:10.1002/brb3.33
84. Pang Y, Cai Z, Rhodes PG (2003) Disturbance of oligodendrocyte development, hypomyelination and white matter injury in the neonatal rat brain after intracerebral injection of lipopolysaccharide. Brain Res Dev Brain Res 140(2):205–214
85. Huleihel M, Golan H, Hallak M (2004) Intrauterine infection/inflammation during pregnancy and offspring brain damages: possible mechanisms involved. Reprod Biol Endocrinol 2:17. doi:10.1186/1477-7827-2-17
86. Beattie MS, Ferguson AR, Bresnahan JC (2010) AMPA-receptor trafficking and injury-induced cell death. Eur J Neurosci 32(2):290–297. doi:10.1111/j.1460-9568.2010.07343.x
87. Bittigau P, Sifringer M, Pohl D, Stadthaus D, Ishimaru M, Shimizu H, Ikeda M, Lang D, Speer A, Olney JW, Ikonomidou C (1999) Apoptotic neurodegeneration following trauma is markedly enhanced in the immature brain. Ann Neurol 45(6):724–735
88. Silverstein FS, Buchanan K, Johnston MV (1986) Perinatal hypoxia-ischemia disrupts striatal high-affinity [3H]glutamate uptake into synaptosomes. J Neurochem 47(5):1614–1619
89. Gallo V, Zhou JM, McBain CJ, Wright P, Knutson PL, Armstrong RC (1996) Oligodendrocyte progenitor cell proliferation and lineage progression are regulated by glutamate receptor-mediated K^+ channel block. J Neurosci 16(8):2659–2670
90. Yuan X, Eisen AM, McBain CJ, Gallo V (1998) A role for glutamate and its receptors in the regulation of oligodendrocyte development in cerebellar tissue slices. Development 125(15):2901–2914
91. Roseth S, Hansen TW, Fonnum F, Walaas SI (1998) Bilirubin inhibits transport of neurotransmitters in synaptic vesicles. Pediatr Res 44(3):312–316
92. Silva R, Mata LR, Gulbenkian S, Brito MA, Tiribelli C, Brites D (1999) Inhibition of glutamate uptake by unconjugated bilirubin in cultured cortical rat astrocytes: role of concentration and pH. Biochem Biophys Res Commun 265(1):67–72. doi:10.1006/bbrc.1999.1646
93. Park E, Velumian AA, Fehlings MG (2004) The role of excitotoxicity in secondary mechanisms of spinal cord injury: a review with an emphasis on the implications for white matter degeneration. J Neurotrauma 21(6):754–774. doi:10.1089/0897715041269641
94. Follett PL, Rosenberg PA, Volpe JJ, Jensen FE (2000) NBQX attenuates excitotoxic injury in developing white matter. J Neurosci 20(24):9235–9241